Title
Engineered jumpers overcome biological limits via work multiplication

Journal
Nature, 604(7907)

ISSN
0028-0836

Authors
Hawkes, Elliot W
Xiao, Charles
Peloquin, Richard-Alexandre
et al.

Publication Date
2022-04-28

DOI
10.1038/s41586-022-04606-3

Engineered jumpers overcome biological limits via work multiplication

Elliot W. Hawkes[1]*, Charles Xiao[1], Richard-Alexandre Peloquin[2], Christopher Keeley[1], Matthew R. Begley[1], Morgan T. Pope[2], & Günter Niemeyer[3]

[1]Department of Mechanical Engineering, University of California, Santa Barbara, CA, USA [2]Disney Research, Pasadena, CA, USA [3]Department of Mechanical and Civil Engineering, California Institute of Technology, CA, USA *email: ewhawkes@ucsb.edu

For centuries, scientists have explored the limits of biological jump height[1,2], and for decades, engineers have designed jumping machines[3–18] that often mimicked or took inspiration from biology. Despite these efforts, general analyses are missing that compare the energetics of biological and engineered jumpers across scale. Here we show how biological versus engineered jumpers have key differences in jump energetics. The jump height of a biological jumper is limited by the work its linear motor (muscle) can produce in a single stroke. In contrast, the jump height of an engineered device can be far greater because its ratcheted or rotary motor can "multiply work" during repeated strokes or rotations. As a consequence of these differences in energy production, biological versus engineered jumpers should have divergent designs for maximizing jump height. Following these insights, we created a device that can jump over 30 m high, far higher than previous engineered jumpers and over an order of magnitude higher than the best biological jumpers. Our work advances the understanding of jumping, shows a new level of performance, and underscores the importance of considering differences between engineered and biological systems.

Introduction

"Jumping [is] a peculiarly attractive subject for investigations," noted preeminent biomechanist R.M. Alexander[19]. It is found across diverse species and size scales, yet is performed in strikingly similar manners and has clear, quantifiable metrics by which ultimate capabilities can be compared: jump height and distance. Indeed, the seemingly simple act of jumping has intrigued thinkers for centuries. Aristotle pondered how humans could increase jump height with halteres[1], while a Renaissance model approximates that all animals, regardless of size, jump roughly the same height of one metre[2]. More recent biological jumper models have examined performance limits across scale in more detail[20], incorporating effects of leg length[19], jumper height[21,22], muscle dynamics[23–25] as well as considering the use of springs[26,27] and latches[28,29] for power-limited jumpers, and air drag for small and light jumpers[11,30]. The performance limits of jumping across scale are thus well-studied, within the domain of biology.

These studies have informed the design of many bio-inspired engineered jumpers, dating back to at least 1967[3]. However, a general modelling framework to capture and quantify inherent differences in biological and engineered jumpers across scale is missing from the literature. Most engineering works focus on specific designs[3–18,31], draw conclusions based on previous biological models[10], or present models that only describe single-stroke linear motors, as found in biology[14,32].

Model

Here we present a model of jumping that compares the energetics of both biological and engineered jumpers. We define a jump as a movement created by forces applied to the ground by the jumper, while maintaining a constant mass (Fig. 1a). Thus, a rocket does not jump, nor does an arrow shot from a bow. We examine two aspects of a jump: specific energy production limits (the maximal energy that could be created for a single jump per unit mass of a jumper) and specific energy utilisation (the efficiency of converting this specific energy into jump height). We concentrate the following discussion on specific energy production limits, as in previous biological studies[26], because we are interested in the upper bounds of jumping, and specific energy directly corresponds to maximum (lossless) jump height in a given gravitational field ($e = gh$). (See Methods: Energy Utilisation Model for discussion of energy utilisation non-idealities such as non-vertical motions[19], distributed mass in the spring[32], and air drag[30].)

For our analysis, we consider the following components of a jumper: a motor, an optional spring, a linkage, and a payload (Fig. 1b). For the motor, we consider two types: biological and engineered (we focus on electromagnetic, though others could be substituted). Both motor types can have one of two transmission types—direct-drive (no spring) or spring-actuated (with spring)—resulting in four jumper configurations. For direct-drive transmissions, the motor directly connects via a stiff, light tendon to a linkage, the structure necessary to transmit forces to the ground. For spring-actuated (also termed power-amplified) transmissions[32–34], the motor may slowly pre-stretch a spring before the spring rapidly releases the energy into the linkage[28]; this can be done without a latch[14,29], but here we focus on the latched case. Finally, the payload comprises all remaining parts of a jumper, including the energy supply (assumed to be sufficient for multiple jumps) and non-energetic items, and we assume the payload does not directly limit or affect the single-jump energy production. We thus consider payload in the Methods: Energy Utilisation Model.

Of the energy-production components, we find the motor to have the most important differences between biological and engineered jumpers. A biological motor is a linear muscle with a finite single stroke bounding its work capacity. An engineered motor, in contrast, can overcome this single-stroke work limit. A linear engineered motor may use ratchets to combine multiple strokes (e.g., in jumping microrobots[35–38]), and a rotary motor may turn repeatedly to combine multiple rotations (e.g., in centimetre-scale robots[13,15]). We term this "work multiplication." The number of strokes or rotations can be raised by increasing the gear reduction between the motor stroke and the jumper's overall motion (see Extended Data Fig. 1). For a direct-drive transmission, work multiplication occurs during the acceleration phase, and for a spring-actuated transmission, it primarily occurs during the pre-stretch phase. Work multiplication is available only to engineered jumpers as ratchets and rotary motors have not been found above the cellular scale in biology[39].

To describe the upper limits of specific energy production, the model considers three primary limiters. The first limiter is the motor's single-stroke specific work[27], or the integral of specific force over stroke length (termed "motor work limiter"). This limiter is not present for engineered jumpers, due to work multiplication. The second limiter is the motor's specific power-time, or the product of specific power and available acceleration time[26] (termed "motor power limiter"). The third limiter is the spring specific energy, or energy that can be stored and released per unit mass of the spring, and it is only present for spring-actuated transmissions (termed "spring energy limiter"). We assume sufficient time between jumps to fully pre-stretch the spring regardless of the motor's power as well as sufficient spring power to discharge the energy during the acceleration time. Additionally, we consider the linkage mass necessary to transfer and apply the energy. Thus, the per-unit-mass specific jumper energy will approach but never reach its bounding limiter, especially at the high specific energies of the best engineered jumpers that require significant linkages (for scaling of linkage mass, see Methods: Energy Production Model).

Model Results and Insights

The results of our model (Fig. 2) show that for biological jumpers, specific energy production can never surpass the motor work limiter, yet for engineered jumpers, the upper bound can be far greater.

Specifically, biological direct-drive jumpers at a large scale (e.g., a leopard) can produce specific energy approaching the motor work limiter; at a small scale (e.g., a lizard), specific energy will be lower due to power limitations[26,27,32]. Biological spring-actuated jumpers at a small scale (e.g., a flea) have sufficient power, but again specific energy is capped by the motor work limiter; at a large scale, springs are unnecessary and actually decrease specific energy due to added mass and muscle-spring force-displacement characteristics[26,27,32]. These trends align with previous models in the literature and biological jump data (Extended Data Fig. 2).

For engineered jumpers, work multiplication eliminates the motor work limiter. At a small scale, spring-actuated transmissions result in higher jumps than direct-drive transmissions, with an upper bound set by the spring energy limiter and the linkage mass. Theoretically, at very large scales, direct-drive transmissions are superior, with an upper bound set by the motor power limiter.

These differences in energetics lead us to find that biological versus engineered jumpers should have divergent designs for maximizing specific energy production—and thus jump height. We present three key insights into these design differences. First, for biological jumpers, the crossover scale below which spring-actuated jumpers produce more specific energy and above which direct-drive jumpers produce more specific energy is approximately 1 m (0.6 s acceleration time). In contrast, for engineered jumpers, this crossover scale is nearly two orders of magnitude larger, at approximately 100 m (3 s acceleration time). (For crossover times, see Fig. 2; for conversion to scale, see Methods: State-space Model and Extended Data Fig. 3-4.)

Second, engineered jumpers should use a ratio of spring mass to motor mass (termed "spring-motor mass ratio") that is much larger than that of biological jumpers (Fig. 2e). In biology, the motor work is the limiting factor; therefore, to maximize specific energy production, the spring energy capacity (i.e., the product of specific energy and mass) should equal but not exceed motor work (See Methods: Spring-motor mass ratio). Since spring specific energy is much larger than motor specific work, only a spring mass much smaller than the motor mass is needed. We find an optimal ratio of 0.029 for biological jumpers, in line with morphological data (0.025-0.06[26]). In contrast, for engineered jumpers with sufficient work multiplication, large amounts of energy can be accumulated in the spring. Thus, we find that the spring-motor mass ratio should be much larger than the ideal ratio for biology. Essentially, work multiplication allows engineering to better utilize the high specific energy of springs.

Third, for spring-actuated transmissions, biological jumpers should maximize the specific work of the motor, but engineered jumpers should maximize the combined specific energy of the spring plus linkage (spring-linkage specific energy). This is because each system should maximize that which primarily limits its specific energy.

From Insights to Jumper Design

We followed these three insights to push the limits of specific energy production, and consequently jump height, for engineered devices with electromagnetic motors. First, we chose a spring-actuated transmission, given the selected scale of 0.3 m. Second, we set a high spring-motor mass ratio by selecting a small rotary motor (10 g) with a large gear reduction (1000:1). This enables the motor to compress a relatively large spring with 150 N of tension in a line wrapped around its spindle (See Methods: Jumper Design). Third, with this peak force constraint, we designed a high-specific-energy hybrid spring-linkage via a custom non-linear simulation framework (See Methods: Jumper Design). We simulated two spring-linkage designs from the literature: a tension linkage[13] (passive carbon fibre linkage with rubber in tension) and a compression bow[10] (carbon fibre only) (Fig. 3a). Our simulation found the tension linkage has only slightly higher specific energy (1,638 J/kg versus 1,313 J/kg), despite the high specific energy of the rubber (7,000 J/kg[40]). To improve, we designed a hybrid-tension-compression spring-linkage, supporting rubber in tension with a compression-bow (1,922 J/kg). The improvement can be thought of in two ways: compared to the tension linkage, we enable the linkage to store energy so it is no longer passive; compared to the compression bow, we add high-specific-energy rubber in tension. Our spring-linkage also has a nearly constant force-displacement curve, which helps it store a large amount of energy given the force constraint. It provides a spring-motor mass ratio (considering the whole spring-linkage mass, 12.4 g) of 1.2 (versus 0.025-0.06[26] in biology).

Using this hybrid spring-linkage and motor design, we created a jumper (Fig. 3b, Extended Data Fig. 5) with minimal losses in six identified stages of energy utilisation (See Methods: Energy Utilisation). For instance, we minimized the mass of the "foot" (components of the jumper that are stationary during acceleration) to make energy transfer losses small, and created a shape-changing morphology that becomes streamlined after take-off to minimize air drag. We measured a payload-free specific energy of 1075 J/kg (24.2 J per 22.5 g, see Methods: Jumper Design), and observed our 30 g jumper accelerating from 0 to over 28 m/s in 9 ms (> 3000 m/s^2) and reaching a height of 32.9 +/- 0.7 m (n = 3) (Fig. 3c).

For comparison, we calculated a payload-free specific energy production for the best biological jumpers of ~170 J/kg[26], and for the best engineered jumpers with electromagnetic motors of ~100 J/kg[15] and ~115 J/kg[13]. Considering payload and other utilisation non-idealities, these specific energies result in jump heights for a galago of 2.25 m[41] and for the engineered jumpers of 3.7 m[15] and 3.8 m[13].

Conclusion

In this work, we presented modelling, insights, and a demonstration. Via modelling, we showed that specific energy production of biological jumpers cannot exceed the motor specific work, yet through work multiplication, engineered jumpers can overcome this limit, resulting in the potential to jump much higher. As a consequence, biological and engineered jumpers have different designs for maximizing specific jump energy—and lossless jump height—which we described in three design insights. According to these, we designed a jumper that demonstrated a jump over 30 m high.

Our model suggests that this is near the feasible limit of jump height with currently available materials. Within specific energy production, assuming that the spring specific energy is near the limit of available materials for solid elastic springs, the primary potential improvement is in the spring-motor mass ratio. However, even increasing the ratio from 1.2 to infinite would only increase jump height by approximately 17% (See Methods: State-space Model, Extended Data Fig. 6). Within specific energy utilisation, the primary improvement comes from minimizing drag effects by increasing scaling; we see less room for improvement in other losses (See Methods: Utilisation Model). However, isometrically scaling the presented jumper by 10x (the predicted optimum which is large enough to eliminate drag but not too large to incur other losses) would result in only a 19% increase in jump height.

Finally, we note that our specialized design trades off adaptability, as found in biology, for high performance. Nevertheless, our results change the implications of jumping as a means of locomotion, changing how and where jumping could be used (see Supplementary Video S4). On Earth, jumping robots could overcome obstacles previously only navigated by flying robots while collecting vision-based data of the ground below (see Supplementary Video S5), and on the Moon, the leaps of the presented jumper would be even loftier: 125 m high while covering half a kilometre in a single bound. Our work fundamentally advances the understanding of the “peculiarly attractive subject” of jumping and underlines the importance of considering the differences between biological and engineered systems.

References:

1. Aristotle. Problemata. in *3* 12–19.
2. Morowitz, H. J. *De motu animalium.* vol. 11 (1976).
3. Seifert, H. S. The lunar pogo stick. *Journal of Spacecraft and Rockets* vol. 4 941–943 (1967).
4. Zhao, J. *et al.* MSU jumper: A single-motor-actuated miniature steerable jumping robot. *IEEE Trans. Robot.* **29**, 602–614 (2013).
5. Niiyama, R., Nagakubo, A. & Kuniyoshi, Y. Mowgli: A bipedal jumping and landing robot with an artificial musculoskeletal system. in *Proceedings - IEEE International Conference on Robotics and Automation* 2546–2551 (2007). doi:10.1109/ROBOT.2007.363848.
6. Scarfogliero, U., Stefanini, C. & Dario, P. Design and development of the long-jumping 'grillo' mini robot. in *Proceedings - IEEE International Conference on Robotics and Automation* 467–472 (2007). doi:10.1109/ROBOT.2007.363830.
7. Li, F. *et al.* Jumping like an insect: Design and dynamic optimization of a jumping mini robot based on bio-mimetic inspiration. *Mechatronics* **22**, 167–176 (2012).
8. Zhao, J., Xi, N., Gao, B., Mutka, M. W. & Xiao, L. Development of a controllable and continuous jumping robot. in *Proceedings - IEEE International Conference on Robotics and Automation* 4614–4619 (2011). doi:10.1109/ICRA.2011.5980166.
9. Churaman, W. A., Currano, L. J., Morris, C. J., Rajkowski, J. E. & Bergbreiter, S. The first launch of an autonomous thrust-driven microrobot using nanoporous energetic silicon. *J. Microelectromechanical Syst.* **21**, 198–205 (2012).
10. Armour, R., Paskins, K., Bowyer, A., Vincent, J. & Megill, W. Jumping robots: A biomimetic solution to locomotion across rough terrain. in *Bioinspiration and Biomimetics* vol. 2 S65 (2007).
11. Bergbreiter, S. Effective and efficient locomotion for millimeter-sized microrobots. in *2008 IEEE/RSJ International Conference on Intelligent Robots and Systems, IROS* 4030–4035 (2008). doi:10.1109/IROS.2008.4651167.
12. Koh, J. S. *et al.* Jumping on water: Surface tension-dominated jumping of water striders and robotic insects. *Science (80-.).* **349**, 517–521 (2015).
13. Woodward, M. A. & Sitti, M. MultiMo-Bat: A biologically inspired integrated jumping-gliding robot. *Int. J. Rob. Res.* **33**, 1511–1529 (2014).
14. Haldane, D. W., Plecnik, M. M., Yim, J. K. & Fearing, R. S. Robotic vertical jumping agility via Series-Elastic power modulation. *Sci. Robot.* **1**, eaag2048 (2016).
15. Zaitsev, V. *et al.* Locust-inspired miniature jumping robot. in *IEEE International Conference on Intelligent Robots and Systems* vols 2015-Decem 553–558 (2015).
16. Kovač, M., Fuchs, M., Guignard, A., Zufferey, J. C. & Floreano, D. A miniature 7g jumping robot. in *Proceedings - IEEE International Conference on Robotics and Automation* 373–378 (2008). doi:10.1109/ROBOT.2008.4543236.
17. Kovač, M., Schlegel, M., Zufferey, J. C. & Floreano, D. Steerable miniature jumping robot. *Auton. Robots* **28**, 295–306 (2010).
18. Burdick, J. & Fiorini, P. Minimalist Jumping Robots for Celestial Exploration. *Int. J. Rob. Res.* **22**, 653–674 (2003).
19. Alexander, R. M. Leg design and jumping technique for humans, other vertebrates and insects. *Philos. Trans. R. Soc. Lond. B. Biol. Sci.* **347**, 235–248 (1995).
20. Alexander, R. M. N. Simple models of human movement. *Appl. Mech. Rev.* **48**, 461–470 (1995).
21. Scholz, M. N., Bobbert, M. F. & Knoek van Soest, A. J. Scaling and jumping: Gravity loses grip on small jumpers. *J. Theor. Biol.* **240**, 554–561 (2006).
22. Cerquiglini, S., Venerando, A., Wartenweiler, J. & Plagenhoef, S. Biomechanics III. in *Medicine & Science in Sports & Exercise* (ed. Hoerler, E.) vol. 6 iv (Karger AG, 1974).

23. Roberts, T. J. & Marsh, R. L. Probing the limits to muscle-powered accelerations: Lessons from jumping bullfrogs. *J. Exp. Biol.* **206**, 2567–2580 (2003).
24. Bobbert, M. F. Effects of Isometric Scaling on Vertical Jumping Performance. *PLoS One* **8**, e71209 (2013).
25. Azizi, E. & Roberts, T. J. Muscle performance during frog jumping: Influence of elasticity on muscle operating lengths. in *Proceedings of the Royal Society B: Biological Sciences* vol. 277 1523–1530 (2010).
26. Bennet-Clark, H. C. Scale effects in jumping animals. *Scale Eff. Anim. Locomot.* **185**, 201 (1977).
27. Sutton, G. P. *et al.* Why do large animals never actuate their jumps with latch-mediated springs? because they can jump higher without them. in *Integrative and Comparative Biology* vol. 59 1609–1618 (2019).
28. Divi, S. *et al.* Latch-based control of energy output in spring actuated systems. *J. R. Soc. Interface* **17**, 20200070 (2020).
29. Longo, S. J. *et al.* Beyond power amplification: Latch-mediated spring actuation is an emerging framework for the study of diverse elastic systems. *Journal of Experimental Biology* vol. 222 jeb197889 (2019).
30. Bennet-Clark, H. C. & Alder, G. M. The effect of air resistance on the jumping performance of insects. *J. Exp. Biol.* **82**, 105–121 (1979).
31. Stoeter, S. A. & Papanikolopoulos, N. Kinematic motion model for jumping scout robots. *IEEE Trans. Robot.* **22**, 397–402 (2006).
32. Ilton, M. *et al.* The principles of cascading power limits in small, fast biological and engineered systems. *Science (80-.).* **360**, eaao1082 (2018).
33. Gabriel, J. M. The effect of animal design on jumping performance. *J. Zool.* **204**, 533–539 (1984).
34. Roberts, T. J. & Azizi, E. Flexible mechanisms: The diverse roles of biological springs in vertebrate movement. *Journal of Experimental Biology* vol. 214 353–361 (2011).
35. Gerratt, A. P. & Bergbreiter, S. Incorporating compliant elastomers for jumping locomotion in microrobots. *Smart Mater. Struct.* **22**, 014010 (2013).
36. Greenspun, J. & Pister, K. S. J. First leaps of an electrostatic inchworm motor-driven jumping microrobot. in *2018 Solid-State Sensors, Actuators and Microsystems Workshop, Hilton Head 2018* 159–162 (2018). doi:10.31438/trf.hh2018.45.
37. Greenspun, J. & Pister, K. S. J. Mechanisms for jumping microrobots. in *International Conference on Manipulation, Automation and Robotics at Small Scales, MARSS 2017 - Proceedings* 1–5 (2017). doi:10.1109/MARSS.2017.8001944.
38. Bergbreiter, S. & Pister, K. S. J. Design of an autonomous jumping microrobot. in *Proceedings - IEEE International Conference on Robotics and Automation* 447–453 (2007). doi:10.1109/ROBOT.2007.363827.
39. Berg, H. C. The rotary motor of bacterial flagella. *Annual Review of Biochemistry* vol. 72 19–54 (2003).
40. Ashby, M. *Materials selection in mechanical design: Fourth edition*. (2010).
41. Hall-Crags, E. C. B. An analysis of the jump of the Lesser Galago (Galago senegalensis). *Proc. Zool. Soc. London* **147**, 20–29 (1965).
42. Josephson, R. K. Contraction dynamics and power output of skeletal muscle. *Annual Review of Physiology* vol. 55 527–546 (1993).
43. Seok, S., Wang, A., Otten, D. & Kim, S. Actuator design for high force proprioceptive control in fast legged locomotion. in *IEEE International Conference on Intelligent Robots and Systems* 1970–1975 (2012). doi:10.1109/IROS.2012.6386252.
44. Miao, Z., Mo, J., Li, G., Ning, Y. & Li, B. Wheeled hopping robot with combustion-powered actuator. *Int. J. Adv. Robot. Syst.* **15**, 1729881417745608 (2018).

45. Ackerman, E. Boston dynamics sand flea robot demonstrates astonishing jumping skills. *IEEE Spectrum Robotics Blog* vol. 2 1 (2012).
46. Dowling, K. Power sources for small robots. (The Robotics Institute, Carnegie Melon University, 1997).

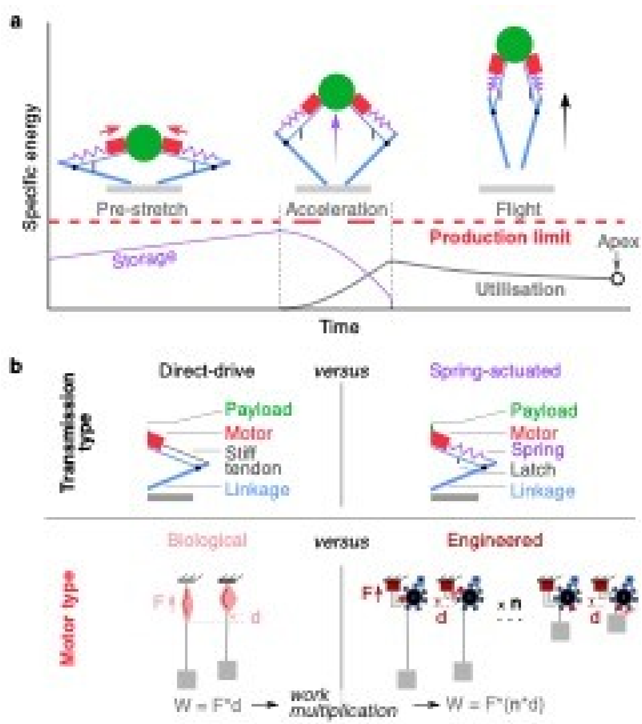

Fig. 1 | Graphical overview of the modelling framework. a, Temporally, we consider a jump to include an optional pre-stretch phase (for jumpers with latched springs), an acceleration phase during which a force is applied to the ground to accelerate the jumper upward, and a flight phase (See SI for details of simulation shown). Energetically, we consider two aspects of a jump. First is the specific energy production limit (red dashed), giving the upper bound on the energy per unit mass that can be produced. Second is the specific energy utilisation (grey curve), considering losses, for example due to non-idealities in energy transfers and air drag (see Methods: Energy Utilisation). Note: only the latched-spring case is shown. **b,** We categorize jumpers according to transmission type (direct-drive versus spring-actuated) and motor type (biological versus engineered). For direct-drive transmissions, the motor connects directly to the linkage, and for spring-actuated transmissions, the motor stretches a spring, which drives the jump. For biological motors (muscles), the output work can never exceed the work of a single stroke. For engineered motors, the output work is the product of the single stroke work multiplied by the number of strokes, termed "work multiplication." Here a ratcheted linear motor is shown; rotary motors perform similarly (Extended Data Fig. 1).

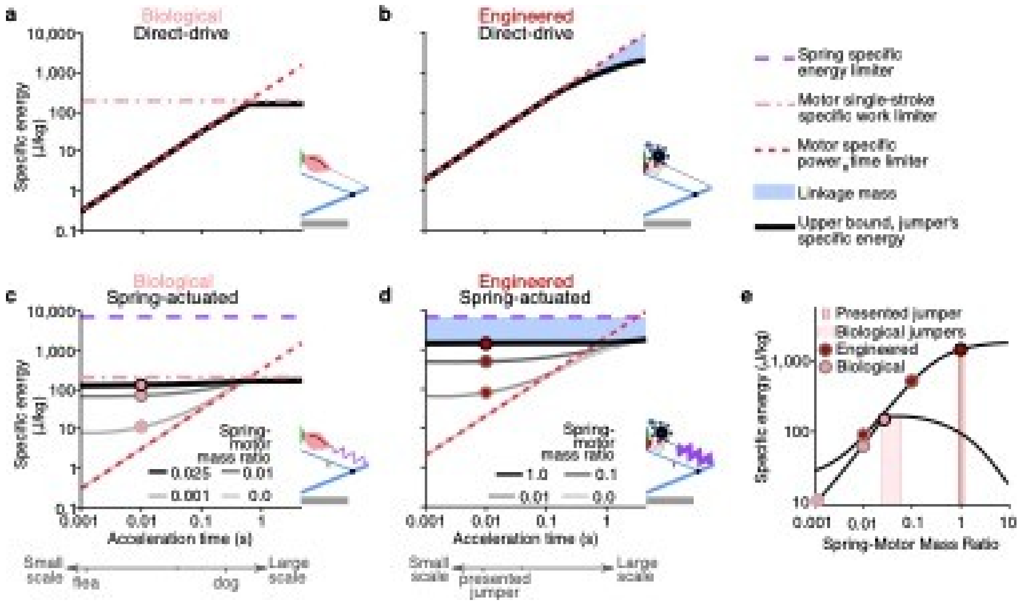

Fig. 2 | Trends of specific energy upper bounds for biological versus engineered, and direct-drive versus spring-actuated jumpers. a-d, The upper bound of a jumper's specific energy (black line) will approach limiters (broken lines), but remain below due to required linkage mass (blue shading). **a,** Biological, direct-drive: two limiters are present, (i) the motor's single-stroke specific work limiter (integral of specific force over stroke length; muscle: ~200 J/kg[26], dash-dot pink), and (ii) the motor's specific power-time limiter (product of specific power (muscle: ~200 W/kg[42]) and acceleration time, dotted red). **b,** Engineered, direct-drive: because work multiplication removes the motor work limiter, only the motor power limiter is present (electromagnetic: ~2000 W/kg[43]). **c,** Biological, spring-actuated: the addition of a latched spring helps overcome the motor power limiter, but adds a new limiter: spring specific energy (tendon/apodeme in pure tension: ~7000 J/kg[26], dashed purple). However, the jumper's specific energy can never surpass the motor work limiter and thus never approaches the spring energy limiter. **d,** Engineered, spring-actuated: work multiplication again removes the motor work limiter, allowing the jumper's specific energy to rise closer to the spring energy limiter (latex in pure tension: ~7000 J/kg[40]). **e,** These differences result in different ideal spring-motor mass ratios (ratio of spring mass to motor mass) in spring-actuated jumpers: ~0.025 for biological and much larger for engineered. Dots in (**c-e**) mark ratio at 0.01 s acceleration time, corresponding to presented jumper. Note: the x-axis for (**a-d**) shows acceleration time, to easily relate power and energy; acceleration time relates monotonically to length scale for an isometrically scaled jumper (see Methods: State-space Model).

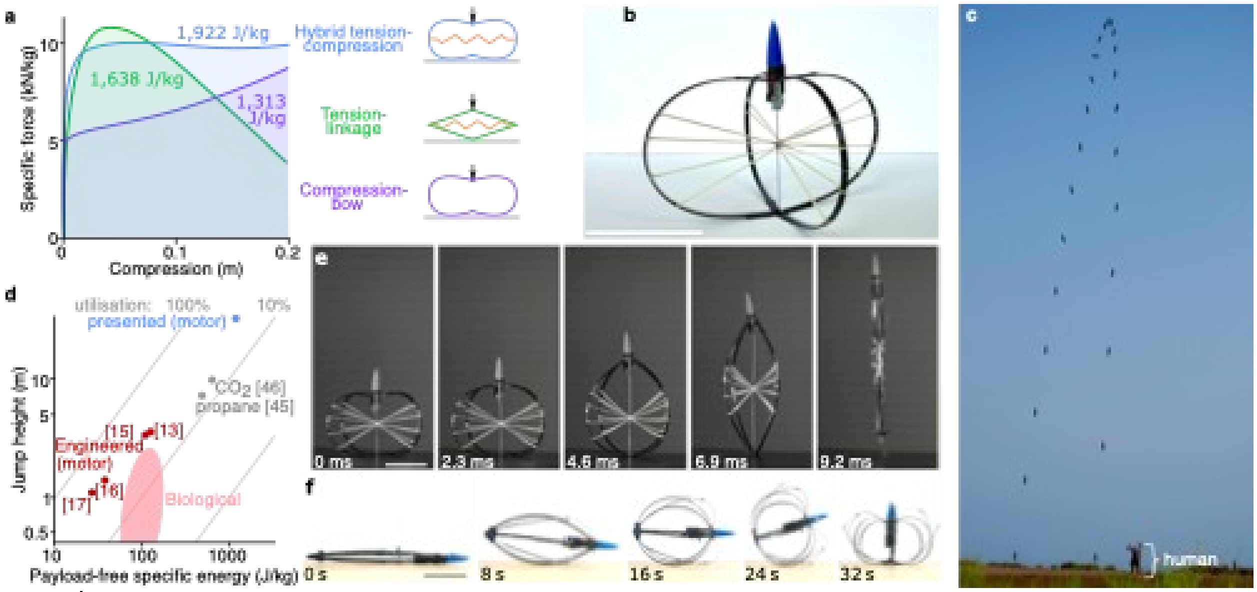

Fig. 3 | From insights to an engineered jumper that exceeds 30 m. a, Simulation results of specific energy (area under curve) for three different spring configurations: two from the literature (tension-linkage[13] and compression-bow[10]) and one that we designed (hybrid tension-compression). **b,** The presented jumper with the hybrid spring in a stable pre-jump configuration. Scale bar 10 cm. **c,** Image of the device jumping with lines added over the position of the jumper every 200 ms (see Supplementary Video S2). Human is 1.83 m. **d,** Jump height of the presented and other jumpers (reference in bracket) shown as a function of the mechanism specific energy (where mechanism is the motor, linkage, and optional spring). Biological jumpers tend to have lower utilisation efficiency (lower jump height for a given mechanism specific energy) due to higher payloads. Two points are shown for jumpers not using electromagnetic motors, but instead propane[44] and CO_2[45] (specific energy of propane is 10,000 kJ/kg[44] and compressed CO_2 in a composite tank is 250 kJ/kg[46]; mechanism specific energy is greatly reduced due to required structure). Grey lines represent energy utilisation. See Extended Data Tables 1 and 2 for details of data and calculations. **e,** Frames from Supplementary Video S1 with acceleration phase occurring in 9 ms. Scale bar: 10 cm. **f,** Frames from Supplementary Video S3 of self-righting using the legs as a roll-cage[10,17], enabled by adding four tapered legs (see Supplementary Video S4 and Methods: Jumper Design for details). Scale bar: 10 cm.

Methods:

Limits of Energy Production Model

We first consider the maximum energy that could be available to the jumper, dependent on its components. We consider the payload, which we assume does not directly limit or affect the single-jump energy production in the Energy Utilisation Model, and segment the remainder of the jumper as follows: (i) a motor, providing the mechanical energy, (ii) optional elastic energy storage or springs, temporarily accumulating mechanical energy, and (iii) inelastic linkage or other elements, applying the energy via ground reaction forces. In the extremes, the jumper may contain no springs (purely inelastic) or it may utilise the springs for structural support and require little to no inelastic linkage elements. Note we include linkage mass in the energy production rather than utilisation, as neither motors nor springs can operate in isolation. Indeed, to fairly evaluate the energy production, we must consider how much linkage mass a design requires to function. We begin with direct-drive transmissions before considering spring actuation. Also note that specific energy per unit mass is denoted by a lowercase e, versus absolute energy is denoted by an uppercase E

Direct-drive Transmission: We determine the maximum specific jump energy, e_{jump}^{direct}, assuming the jumper contains only a motor of mass m_m and a linkage of mass m_l. In biology, the muscle's specific energy is limited by the maximum specific work of a full stroke

$$e_m^{bio} = \frac{1}{m_m} \int_0^d F_{max}\, dx$$

defined by integrating the maximum force, F_{max}, over the entire stroke, d. In engineering, a linear motor with the addition of a ratchet could complete multiple strokes to overcome such a limit. Similarly, a rotary motor has an unlimited stroke and hence an unlimited energy (limited ultimately only by the energy supply; because battery specific energy is orders of magnitude larger than those considered in this analysis, approximately 500 kJ/kg[46], we assume it is nearly infinite). We generally apply

$$e_m^{eng} = \infty \, .$$

Interestingly, biological muscle ratchets at a microscopic scale, but its macroscopic structure loses the feature and limits its stroke.

Both biological and engineered motors are also limited by their maximum specific power $p_m = \frac{P_m}{m_m}$, available during the acceleration time t_0. The specific jump energy is thus limited by both as

$$e_{jump}^{\text{direct}} = \frac{E_{jump}^{\text{direct}}}{m_m + m_l} = \frac{\text{Min}\left(E_m, P_m t_0\right)}{m_m + m_l} = \frac{\text{Min}\left(m_m e_m, m_m p_m t_0\right)}{m_m + m_l} = \frac{m_m}{m_m + m_l} \text{Min}\left(e_m, p_m t_0\right)$$

Spring-actuated Transmission: We further include a spring of mass m_s, with a maximum specific energy capacity of $e_s = \frac{E_s}{m_s}$. If we allow the motor a pre-stretch time t_p, the spring may store energy up to

$$E_{store} = \text{Min}\left(m_s e_s, m_m e_m, m_m p_m t_p\right)$$

If we allow the motor to continue providing energy during the acceleration phase (not possible for many jumper designs, but represents the upper limit) and assume the spring can deliver specific power up to $p_s = \frac{P_s}{m_s}$, we have a maximum specific jump energy of

$$e_{jump}^{\text{spring}} = \frac{E_{jump}^{\text{spring}}}{m_m + m_s + m_l} = \frac{\text{Min}\left[m_m e_m, E_{store} + m_m p_m t_0, m_s p_s t_0\right]}{m_m + m_s + m_l}$$

Finally, if we assume the spring's output specific power p_s far exceeds the requirements $p_s \gg \frac{e_s}{t_0}$, we find

$$e_{jump}^{\text{spring}} = \frac{E_{jump}^{\text{spring}}}{m_m + m_s + m_l} = \frac{\text{Min}\left[m_m e_m, m_m p_m (t_p + t_0), m_s e_s + m_m p_m t_0\right]}{m_m + m_s + m_l}$$

Spring-Motor Mass Ratio: The mass ratio is used in Fig. 2. We see that increasing the spring mass m_s only helps when the system is neither limited by motor energy nor by motor power

$$e_{jump}^{\text{spring}} = \frac{m_m}{m_m + m_s + m_l} \text{Min}\left[e_m, p_m (t_p + t_0), \frac{m_s}{m_m} e_s + p_m t_0\right]$$

Thus, assuming sufficient pre-stretch time t_p, biological jumpers are helped up to an optimal mass ratio where $e_m = \frac{m_s}{m_m} e_s + p_m t_0$, or

$$\left(\frac{m_s}{m_m}\right)_{optimal} = \frac{e_m - p_m t_0}{e_s} \approx \frac{e_m}{e_s},$$

which equates to ~0.029 when values of e_m and e_s from Fig. 2 are used (~200 J/kg and ~7000 J/kg, respectively). In contrast, adding spring mass to engineered jumpers helps indefinitely, approaching the maximal specific energy

$$\left(e_{jump}^{\text{spring}}\right)_{limit} = \frac{m_s e_s + m_m p_m t_0}{m_m + m_s + m_l} \rightarrow \frac{m_s}{m_s + m_l} e_s,$$

assuming the linkage mass m_l also needs to increase to support the higher energies.

Size/Length Scaling: Beyond mass ratios, the jump energy limit only depends on the motor/spring specific energy/power properties, as well as the pre-stretch time (which we assume can be freely selected) and the acceleration time, t_0. The specific energies and powers are assumed to be scale-invariant: in biology[47,48], muscle forces scale with area, $F_{max} \propto L^2$, while distance (stroke) and velocity scale with length, $d \propto L$, $v_{max} \propto L$, and mass scales with volume, $m \propto L^3$. In engineering, with electromagnetic rotary motors, the torque scales with the 4th power of length, $\tau \propto L^4$, while angular speed scales inverse linearly, $\omega \propto L^{-1}$, so again the power remains scale invariant[47,49,50]. Similar to biological muscle, all spring forces scale with area, $F_{max} \propto L^2$, while distances (stroke) scale with length, $d \propto L$, such that spring specific energies are scale independent.

We also note that assume the required linkage mass m_l simply scales with jump energy: to maintain a constant stress across scale, the cross-sectional area of the linkage will scale with force F_{max}, while the length scales with stroke d. As such, we can define a scale-invariant specific energy transfer capacity

$$e_l = \frac{E_{jump}}{m_l}.$$

Equivalently, and again assuming sufficient pre-stretch time t_p, we write the required linkage mass as

$$m_l = \frac{E_{jump}}{e_l} = \frac{\mathrm{Min}\left[m_m e_m,\, m_s e_s + m_m p_m t_0\right]}{e_l}$$

to obtain

$$e_{jump} = \frac{E_{jump}}{m_m + m_s + m_l} = \frac{1}{\dfrac{1+\dfrac{m_s}{m_m}}{\mathrm{Min}\left[e_m, \dfrac{m_s}{m_m} e_s + p_m t_0\right]} + \dfrac{1}{e_l}}.$$

For a spring-actuated engineered jumper, this brings the maximal specific energy for an infinite spring-motor mass ratio to

$$\left(e_{jump}\right)_{eng-limit} = \frac{1}{\dfrac{1}{e_s} + \dfrac{1}{e_l}} = \frac{e_s e_l}{e_s + e_l}.$$

We note that this final expression is similar to how stiffnesses of springs add in series. In Fig. 2, we approximate for engineering e_l as 2650 J/kg, based on the values from our jumper (where $e_s = 7000\,\frac{J}{kg}$ and $\left(e^{\text{spring}}_{jump}\right)_{limit} = 1922\,\frac{J}{kg}$). For a motor-work-limited biological jumper with minimal spring mass, we calculate

$$\left(e_l\right)_{bio} = \frac{e_m m_m}{m_l},$$

as 1130 J/kg, based on the values for muscle specific energy (200 J/kg) and percent of mass of the skeleton (~14%[51]).

Only the acceleration time t_0 is scale dependent (for both direct-drive and spring-actuated transmission types). For isometric scaling assumptions, acceleration time monotonically increases with scale. More specifically, for all but the largest direct-drive jumpers, configured to operate at peak power during the entire acceleration phase, time scales with a $2/3$ power, $t_0 \propto L^{2/3}$ (see State-space Model below and previous biological model[26]). Meanwhile, the acceleration time for spring-actuated jumpers increases linearly with scale, $t_0 \propto L$ (also see State-space Model below).

We finally note that our model showing that spring-powered jumpers are scale-invariant in specific energy production contrasts with the conclusions of previous work[32], which stated that specific energy production decreases at small scales for spring-powered jumpers. The discrepancy arises from differing model assumptions: the previous work, in an effort to model not just jumpers but also many other high-power movements, considered a catapult launching a projectile, where only the projectile, but not the catapult, changed size during scaling. This led to the conclusion that the catapult's spring would meet material limits; however, during scaling of a jumper, spring and all, this effect is not present, and spring-powered biological jumpers should be scale-invariant, as shown in more recent work[27].

Energy Utilisation Model

An energy utilisation model is a helpful design tool, as it describes the effects of different losses on the achievable jump height, h, (defined as the change in vertical COM position from standing to apex), given a maximum payload-free specific jump energy, e_{jump}. Using an energy flow perspective, we lump all losses and reductions into the following six types or stages. We note that many of the individual components have been discussed in separate papers, as referenced below, and that this general framework that assembles disparate models is helpful for design and analysis. Further, we realize the numerical computation of each reduction may require assumptions or approximations (see the Supplementary Information for derivations). The six stages are:

	Specific Energy			*Losses*
1	Produced Energy:	$e_{\prod ¿¿}$ ¿	$e_{jump}^{□} \eta_{\prod ¿¿}$	*(production inefficiency)*
2	Available Energy:	e_0 ¿	$e_{\prod ¿\left(1-\frac{m_{payload}}{m}\right)¿}$	*(payload apportionment)*
3	KE, Total:	e_{KE} ¿	$e_0 - Lg\frac{m_{body}}{m}$	*(less energy-to-stand)*
4	KE, Vertical:	e_{vert} ¿	$e_{KE}\left[1-\beta_{xy}-\beta_{\theta}\right]$	*(less non-vertical)*
5	KE, Centre of Mass:	e_{COM} ¿	$e_{vert}\left[1-\frac{m_{foot}}{m}\right]$	*(less energy transfer losses)*
6	PE, Centre of Mass:	e_{apex} ¿	$e_{COM}\left[1-\frac{D_s e_{COM}}{2}\right]$	*(less aerodynamic drag)*

Where $\eta_{\prod ¿¿}$ is production efficiency, $m_{payload}$ is the mass of the payload, m is the total mass, m_{body} is the lumped mass that is moving during acceleration (see SI), m_{foot} is the lumped mass that is static, β_{xy} and β_{θ} are the fraction of the kinetic energy due to movements in any horizontal direction and due to rotations, respectively, and D_s is a drag constant (see SI). Overall, we write the model as

$$h=\frac{1}{g}e_{apex}=\frac{1}{g}¿$$

Further details of each stage:

1) Produced specific energy, $e_{\prod ¿¿}$, considering the production efficiencies: Any impedance mismatches between components or viscous losses will reduce the available energy. Practically, the force-displacement profiles of biological muscle and tendons limits jumpers to obtain 30-50% of the potential muscle energy[26,27]. In contrast, our nearly constant force spring matches the nearly constant force output of our motor, mitigating this loss. Further, a very small damping ratio (0.02) was experimentally determined for the carbon fibre experimentally measured using a clamped beam oscillation method[52].

2) Initial specific energy before movement, e_0, that can be released in a single jump: Any payload requires apportionment across the entire mass[26]. Our jumper has a payload-free mass of 22.5 g and payload mass of only 7.9 g. Thus the 1075 J/kg payload-free specific energy is reduced to 796 J/kg in this step. However, we see little room for improvement here. Our battery is a lithium polymer battery, which is the lightest commercially available option. Our release mechanism has a mass of 1.23 g (made from 7075 aluminium) and our nose cone 1.2 g. All other components are less than a gram.

3) Total specific kinetic energy, e_{KE}, after the full stroke has occurred: This deducts the potential energy surrendered to raise the centre of mass from crouch to stand[21]. This delivers the jump height as the

change in height of the centre of mass above its position when the jumper is fully standing. Our jumper has negligible loss here, due to its small size and high jump.

4) Vertical specific kinetic energy, e_{vert}, due to movements in the vertical (z) direction only[19]. This deducts the fraction of the kinetic energy due to movements in any horizontal direction (β_{xy}) and due to rotations (β_{θ}). This also includes potential losses due to sliding on the ground surface or frictional losses in joints. Along with (5), below, our jumper has roughly 50% efficiency for these stages. Interestingly, a pure compression spring of a solid material with only vertical motion mitigates this non-vertical loss, but is only 50% for the energy transfer loss. Alternatively, a realistic compression spring, such as a coil or bow spring, will have substantial non-vertical motion, meaning its efficiency will be below 50%. Our device exceeds 50% because of its payload, which is placed at the top of the jumper, while the "foot" mass is minimized (only the bottom of the spring).

5) Vertical Centre-Of-Mass (COM) specific kinetic energy, e_{COM}, after launch: This deducts the transfer losses shifting energy from individual masses to the COM motion[18,19,32]. It effectively removes energy of internal relative motions, accelerating the foot and the portion of the spring that was stationary prior to launch.

6) Potential energy at the jump apex, e_{apex}: This deducts the aerodynamic drag losses occurring during the jump[11,30]. Our jumper loses about 25% of its energy due to air drag, even with its highly streamlined body. This loss is possible to mitigate by scaling 10x (Extended Data Fig. 6).

Regarding isometric scaling, we note the energy-to-stand losses dominate at large scales. For any jumper with a scale-invariant maximum jump energy, we find a maximum standing height

$$L_{stand}=\frac{1}{g}\frac{m-m_{payload}}{m-m_{foot}}\eta_{\prod} ¿ e_{jump} ¿$$

beyond which jumping is no longer possible. Meanwhile, at small scales the aerodynamic losses dominate. See State-space Model and Supplementary Information, Energy Utilisation Model for further details.

State-space Model: Adding Jumper Specifics

We also simulate jumpers using a simple 2nd-order model. Assume a single moving lumped body mass, m_b, with vertical position z, velocity v, acceleration a, consistent with previous jumping models[32]. The jumper has a length scale, L, which we define as the leg stroke, or difference between the body height when the jumper is fully crouched ($z=0$) and when standing ($z=L$ ¿; the jump height is measured above $z=L$. This model neglects the effects of geometric linkages, motor internal inertias, multiple masses, etc., but captures the fundamental power and energy production and predicts acceleration times relative to the jumper scale. We consider direct-drive and spring-actuated transmissions.

Direct-drive Transmission: Assume the body is driven, via a reduction G, by an inertia-free motor with linear viscous losses:

$$m_b a = G F_m\left(1-\frac{Gv}{v_m}\right)-m_b g$$

where F_m and v_m are the motor's maximum force and velocity respectively. We consider both fixed reductions and variable reductions, where the motor continually operates at maximum power. The latter case is modelled by

$$m_b a=\frac{F_m v_m}{4v}-m_b g=\frac{m_m p_m}{v}-m_b g$$

We again note biological and engineered motor specific power is scale invariant[47,49,50]

$$p_m=\frac{F_m v_m}{4m_m}=\text{constant}.$$

For biological jumpers, assume G is upper-bound by a value of one, in the case when the muscle completes a full stroke during the leg stroke. Consequently, the scale-invariant motor specific energy is

$$e_m^{bio}=\frac{F_m L}{m_m}=\text{constant} \quad .$$

We simulate a payload-free system using the same motor parameters as described in Fig 2. The body mass is composed of the motor and linkage mass such that $m_b=m_s+m_l$. Extended Data Fig. 3 graphs the results.

Not surprisingly, operating at maximum power, when possible, delivers the most energy. It also provides acceleration times scaled with a 2/3 power of size. We further note that biological jumper's finite motor stroke limits both maximum power operation and the reduction, such that large scale animals have limited energy and see a drop off in their kinetic energy due to increasing energy to stand, ultimately limiting the size of animals that can jump. In contrast, linkage-less engineered jumpers theoretically can produce more energy the larger they are (Extended Data Fig. 3a); when the energy to stand is considered, the kinetic energy eventually plateaus (Extended Data Fig. 3b).

Spring-actuated Transmission: Alternatively, assume the motor pre-stretches a latched linear spring linkage assembly of additional mass m_s. In turn, when fully stretched and released, the spring propels the body upward. If the spring shows uniformly distributed mass and uniform strain rate, then effectively $\frac{1}{2}m_s$ contributes to potential energy, while $\frac{1}{3}m_s$ contributes to kinetic energy. We can thus model

$$\left(m_b+\frac{1}{3}m_s\right)a=k(L-z)-\left(m_b+\frac{1}{2}m_s\right)g$$

where the stiffness, k, relates to the effective spring specific energy

$$e_s=\frac{\frac{1}{2}kL^2}{m_s}$$

This implicitly maps the appropriate portion of the spring to the foot and body. We again simulate the system using the spring specific energy from Fig. 2 and assume the body mass consists of only a motor mass. We then vary the effective spring-motor mass ratio.

Extended Data Fig. 4 shows the results. Note, for such spring-actuated jumpers, the acceleration time increases linearly with scale. We also see that smaller springs impose a limit on the size of jumper – smaller spring forces cannot overcome larger weights. And naturally, smaller springs provide less energy, specific to the total jumper mass.

A more detailed description of state space model is found in the Supplementary Information.

Jumper Design:

Spring Material Selection: We search a material database to maximize the "material factor," or the ratio of the elastic stored energy during axial extension to mass:

$$\kappa = \frac{\sigma_y^2}{E\rho},$$

where σ_y is the yield stress, E is the modulus of elasticity, and ρ is the density (Extended Data Fig. 5a). The largest material factor occurs among two main groups of materials: elastomers at lower values of E/ρ (we choose latex rubber), and fibre-reinforced composites at higher values of E/ρ (we choose carbon-fibre composite). See SI for further details.

Spring Design: To explore the design space of springs, we built a non-linear quasistatic simulation framework, comparing the three designs outlined in the main text. The simulation provides a guideline for selecting spring parameters for designing a hybrid spring, suggesting ratios of rubber cross-section to length for a given carbon-fibre cross section to length, such that peak strain in the carbon-fibre is reduced compared to the no-rubber case. See SI for details of the simulation and comparison.

Jumper Design: A small highly geared motor reels in an ultra-high-molecular-weight polyethylene line (Spectra) to compress the spring, storing ~24.2 J of energy at a stress of >90% of the bow ultimate strength. A lightweight release mechanism unlatches to relieve the tension in the line and initiate a jump (see Extended Data Fig. 5). We mount the motor, this release mechanism, the batteries and the nose cone at the top of the bows. Placing as much of the necessary mass on the moving body helps reduce the foot mass ratio and improves the energy transfer in stage 4 of the energy utilisation model.

We power the motor using a small lithium polymer cell battery (enough energy for roughly 10 jumps). The battery is packaged in a model rocket nose cone which helps reduce the drag of the jumper. To further reduce drag, the robot shape-changes during the acceleration phase, from a wide, stable configuration to a streamlined, rocket-like shape (See Supplementary Videos S6-S7). Cyanoacrylate adhesive is used throughout for bonding. The combination of a lightweight construction and high-strength materials means the jumper can survive landing on even concrete surfaces from its apex height of over 30 m. All of the components are shown in Extended Data Fig. 5d and listed in Extended Data Table 3.

Release Mechanism: The goals of the release mechanism are to quickly release tension in the string that compresses the bow spring (extension of the spring occurs in less than 9 ms), enable resetting for another jump, manage the high forces (~130 N), and be as light as possible. This is achieved with a hinged arm that supports a roller, which turns on bearings, and over which the string passes (Extended Data Fig. 5c). A latch opens to release the tension from the string, after which a rubber band resets the arm, allowing the motor to begin winding for another jump without ever stopping. Given the small size of the motor, reset time is roughly 2 minutes. This could be decreased by increasing the motor size (e.g., doubling the motor mass (and power) would approximately halve reset time).

Self-Righting Mechanism: To right between jumps, a simple modification to the jumper can be made: adding four bows, one between each set of the main bows, that are tapered and split such that they have an asymmetric shape when compressed (Extended Data Fig. 5e, Fig. 3f). The concept of a roll-cage has been employed previously for self-righting[10,17]. In the presented design, the tapered and split bows contact the ground and deform during compression to push the jumper upright. (See Supplementary Video S3.)

Determining Jumper's Payload-free Specific Energy: This value can be determined as the energy the motor is able to store in the spring-linkage per mass of the motor and spring-linkage. A force-displacement curve was measured for the hybrid compression-tension spring, using the displacement that the motor is able to create (20.3 cm) (Extended Data Fig. 5b). The stored energy is measured as 24.2 J, the hybrid spring-linkage mass as 12.4 g, and motor mass as 10.1 g; thus, we find an overall payload-free specific energy of 1075 J/kg.

Code availability. MATLAB code for energy production and utilization models and state-space model, as well as spring simulation, are available upon request.

Data availability. All data is available in Extended Data Tables 1-3.

Methods and Extended Data Figure References:

47. Marden, J. H. & Allen, L. R. Molecules, muscles, and machines: Universal performance characteristics of motors. *Proc. Natl. Acad. Sci. U. S. A.* **99**, 4161–4166 (2002).
48. Hirt, M. R., Jetz, W., Rall, B. C. & Brose, U. A general scaling law reveals why the largest animals are not the fastest. *Nat. Ecol. Evol.* **1**, 1116–1122 (2017).
49. Winslow, J., Hrishikeshavan, V. & Chopra, I. Design methodology for small-scale unmanned quadrotors. in *Journal of Aircraft* vol. 55 1062–1070 (2018).
50. Dermitzakis, K., Carbajal, J. P. & Marden, J. H. Scaling laws in robotics. in *Procedia Computer Science* vol. 7 250–252 (2011).
51. Mitchell, H. H., Hamilton, T. S., Steggerda, F. R. & Bean, H. W. the Chemical Composition of the Adult Human Body and Its Bearing on the Biochemistry of Growth. *J. Biol. Chem.* **158**, 625–637 (1945).
52. Hunt, J. F., Zhang, H., Guo, Z. & Fu, F. Cantilever beam static and dynamic response comparison with mid-point bending for thin mdf composite panels. *BioResources* **8**, 115–129 (2013).
53. Parry, D. A. & Brown, R. H. J. The Jumping Mechanism of Salticid Spiders. *J. Exp. Biol.* **36**, 654–664 (1959).
54. Marsh, R. L. & John-Alder, H. B. Jumping performance of hylid frogs measured with high-speed cine film. *J. Exp. Biol.* **188**, 131–141 (1994).
55. Evans, M. E. G. The jump of the click beetle (Coleoptera, Elateridae)—a preliminary study. *J. Zool.* **167**, 319–336 (1972).
56. Brackenbury, J. & Hunt, H. Jumping in springtails: mechanism and dynamics. *J. Zool.* **229**, 217–236 (1993).
57. Maitland, D. P. Locomotion by jumping in the Mediterranean fruit-fly larva Ceratitis capitata. *Nature* **355**, 159–161 (1992).
58. Harty, T. H. Jump energetics and elastic mechanisms in the pacific jumping mouse (Zapus trinotatus). *Oregon State University* (2010).
59. Schwaner, M. J., Lin, D. C. & McGowan, C. P. Jumping mechanics of desert kangaroo rats. *J. Exp. Biol.* **221**, jeb186700 (2018).
60. Katz, S. L. & Gosline, J. M. Ontogenetic Scaling of Jump Performance in the African Desert Locust (Schistocerca Gregaria). *J. Exp. Biol.* **177**, 81–111 (1993).
61. Toro, E., Herrel, A., Vanhooydonck, B. & Irschick, D. J. A biomechanical analysis of intra- and interspecific scaling of jumping and morphology in Caribbean Anolis lizards. *J. Exp. Biol.* **206**, 2641–2652 (2003).
62. Essner, R. L. Three-dimensional launch kinematics in leaping, parachuting and gliding squirrels. *J. Exp. Biol.* **205**, 2469–2477 (2002).
63. Gregersen, C. S. & Carrier, D. R. Gear ratios at the limb joints of jumping dogs. *J. Biomech.* **37**, 1011–1018 (2004).
64. Burrows, M. & Dorosenko, M. Jumping mechanisms and strategies in moths (Lepidoptera). *J. Exp. Biol.* **218**, 1655–1666 (2015).
65. Bobbert, M. F., Gerritsen, K. G. M., Litjens, M. C. A. & Van Soest, A. J. Why is countermovement jump height greater than squat jump height? *Med. Sci. Sports Exerc.* **28**, 1402–1412 (1996).
66. Brackenbury, J. & Wang, R. Ballistics and visual targeting in flea-beetles (Alticinae). *J. Exp. Biol.* **198**, 1931–1942 (1995).
67. Burrows, M. Jumping performance of froghopper insects. *J. Exp. Biol.* **209**, 4607–4621 (2006).

Acknowledgements We thank W. Heap for assistance with jumper design and testing, K. Chen for assistance testing jumpers, F. Porter for assistance with modelling, H. Bluestone for editorial suggestions., G. Hawkes for early discussions on the limits of jumping, S. Rufeisen and K. Park for help filming, A. Sauret for sharing high-speed videography equipment, and K. Fields for technical support. This work was partially supported by was supported by an Early Career Faculty grant from NASA's Space Technology Research Grants Program.

Author contributions E.H., M.P., and G.N. designed the research; E.H., R.P., and C.K. performed the experiments; E.H., M.P., G.N., C.K., C.X. and R.P. analysed the data; C.X., M.B., and G.N. performed modeling and simulations; C.K., R.P., and E.H. built the jumpers; E.H., G.N., and C.X. wrote the paper; E.H., M.P., and G.N. supervised the project.

Competing interests The authors declare no competing interests.

Additional information

Extended data is available for this paper at

Supplementary information is available for this paper at

Reprints and permissions information is available at http://www.nature.com/ reprints.

Correspondence and requests for materials should be addressed to E.H.

Publisher's note: Springer Nature remains neutral with regard to jurisdictional claims in published maps and institutional affiliations.

Extended Data Fig. 1 | Work multiplication in more detail. a, Similar to a ratcheted motor in Fig. 1, a rotary motor can accomplish work multiplication through multiple rotations instead of multiple strokes. **b,** The output work of a biological jumper is determined by fixed parameters (motor stroke, leg stroke, and motor force), but work multiplication overcomes this for engineered jumpers: For biological jumpers, motor stroke and leg stroke determine an effective gear ratio, if the entire stroke of both is to be used (in animals, the gear ratio varies around this value slightly throughout the jump[19]). With this determined gear ratio and a fixed motor force (assuming a size of motor), the leg force is determined. Finally, with the fixed leg stroke and determined leg force, the output work is determined. In contrast, for engineered jumpers, although the leg stroke is roughly fixed (assuming a size of jumper), the motor can make multiple strokes or rotations, allowing the gear ratio to be designed (higher gear ratio will result in more strokes, at the cost of more time). With this designed gear ratio and a fixed motor force (assuming a size of motor), the leg force is also multiplied with respect to the leg force in the single-stroke case. Finally, with the fixed leg stroke and the multiplied leg force, the output work is also multiplied.

Extended Data Fig. 2 | Biological mechanism specific energy data. The model (Fig. 2a,c) predicts an upper limit to specific energy for all biological jumping mechanisms, regardless of transmission type, at approximately 200 J/kg (dash-dot green). Across scales found in nature, this limit holds. Note that the energy utilisation was estimated at 15%, similar to previous biological work[26,27]. However, variation likely occurs, with jumpers with higher take-off velocities likely having more mass dedicated to jumping muscles, and thus having a higher energy utilisation efficiency. A higher utilisation efficiency, e.g. 30%, would result in a lower mechanism specific energy than shown here. The model also predicts a limit due to motor specific power. Direct-drive jumpers fall on or below this limit (dashed blue). Non-latched spring-actuated jumpers can exceed this limit, and latched spring-actuated jumpers can exceed it by even greater amounts (distance from blue dashed line). However, all still fall below. See Extended Data Table 1 for data.

Extended Data Fig. 3 | Direct-actuated jumper simulations. a, The produced energy specific to the jumper mass. **b,** The centre-of-mass kinetic energy, specific to the jumper mass. **c,** The acceleration time. **d,** The optimal fixed reduction, G, producing the highest acceleration velocity for each jumper scale. The simulations are performed (i) for biological jumpers with fixed reductions of 0.01, 0.1, and 1 (dotted lines), and (ii) for biological jumpers (blue solid) and engineered jumpers (red solid: no linkage; red dotted: with linkage) using variable reduction to operate at maximum power. Each fixed reduction is only possible up to a limiting scale, where the motor force balances the body weight. Biological jumpers operating at full power are also limited in scale, as the motor runs out of stroke. Consequently, biological energy production is always limited by the motor energy (black dashed line). Finally, when operating at the optimal fixed or full-power variable reduction, the acceleration time scales with a 2/3 power of size, reflected in the same scaling in energy and gear reduction.

Extended Data Fig. 4 | Spring-actuated engineered jumper simulations. **a,** The produced energy specific to the jumper mass. **b,** The centre-of-mass kinetic energy, specific to the jumper mass. **c,** The acceleration time. The simulations are performed for spring mass ratios of ranging from 0.001-10. A lower mass ratio lowers the produced energy specific to the total mass and also imposes an upper bound on size, as smaller springs cannot match larger weight forces. The acceleration time scales nearly linearly with the size, and bigger springs create faster jumps.

Extended Data Fig. 5 | Jumper design details. a, Ashby plot of materials with the largest material factor, or the square of yield strength over density. At low elastic moduli are elastomers, but these require a passive linkage to load in tension. At high elastic moduli are fibre-reinforced composites, which can act as stand-alone compression bow springs, but have lower specific energies than elastomers in tension. We therefore design a hybrid spring with elastomer in tension and carbon fibre in bending, replacing the passive linkage. **b,** Force-displacement plot of our hybrid linkage-spring, with total area under the curve (energy) shown. **c,** Schematic and pictures of the minimalistic release mechanism for unlatching. During winding of the string, the motor shaft turns, pulling the string over a shaft supported by bearings in the arm and compressing the hybrid spring-linkage. With further winding, a lever on the string eventually hits the latch, prying it open. The arm swings open, allowing the string to unspool from the shaft. **d,** Components of the jumper before assembly. **e,** Self-righting mechanism. Without a self-righting mechanism, the top-heavy jumper will roll nose-down during compression of the bow springs, given its mass distribution. However, if tapered and split bows are added between each pair of the main, non-tapered bow springs, the behaviour can be reversed. The taper in the bow near the nose creates a high radius of curvature during compression, contacting the ground and forcing the nose to roll upward. The split section continues this as the jumper nears completion of the righting behaviour.

Extended Data Fig. 6 |Simulating presented jumper across spring-motor mass ratio and scale. Using the state-space model modified with the specifics of the presented jumper, we simulated jump height. We included both energy production and energy utilisation. When the spring-motor mass ratio is increased to infinite, we see only a 17% increase in jump height (from 32.9 to 38.6 m). When the scale is increased by 10x, we find an increase of only 19% in jump height (from 32.9 to 39.1 m). The star denotes the presented jumper (0.3 m scale, 32.9 m jump height).

Extended Data Fig. 7 |Schematic of simplified jumper. a, Schematic of jumper used in the Fig. 1a. **b-d,** Free body diagrams of the body, top linkage, and bottom linkage, respectively.

Extended Data Table 1: Biological jump data.

Extended Data Table 2: Engineered jumper data. Mechanism specific energy is calculated as the energy production divided by the mass of the mechanism (motor, spring, and linkage). The "~" represents numbers estimated from source.

Extended Data Table 3: Jumper specifications.